Eur J Vasc Endovasc Surg (2016) 51, 518–526

Positron Emission Tomography and Magnetic Resonance Imaging of Cellular Inflammation in Patients with Abdominal Aortic Aneurysms

O.M.B. McBride [a,b,c,*,e], N.V. Joshi [a,b,c,e], J.M.J. Robson [a,b,c], T.J. MacGillivray [b], C.D. Gray [b], A.M. Fletcher [b], M.R. Dweck [a,b,c], E.J.R. van Beek [a,b], J.H.F. Rudd [d], D.E. Newby [a,b,c], S.I. Semple [b]

[a] Centre for Cardiovascular Science, University of Edinburgh, Edinburgh, UK
[b] Clinical Research Imaging Centre, University of Edinburgh, Edinburgh, UK
[c] Royal Infirmary of Edinburgh, Edinburgh, UK
[d] Division of Cardiovascular Medicine, University of Cambridge, Cambridge, UK

WHAT THIS PAPER ADDS

Comparing these techniques identifies a modest correlation but some key differences related to the spatial distribution of ^{18}F-FDG and USPIO uptake. This may reflect the differing elements of macrophage activity detected by these modalities: glycolysis and phagocytosis. Further studies are needed to assess whether identification of this varying activity will influence aneurysm growth rates and the clinical outcome.

Objectives: Inflammation is critical in the pathogenesis of abdominal aortic aneurysm (AAA) disease. Combined ^{18}F-fludeoxyglucose (^{18}F-FDG) positron emission tomography with computed tomography (PET-CT) and ultrasmall superparamagnetic particles of iron oxide (USPIO)-enhanced magnetic resonance imaging (MRI) are non-invasive methods of assessing tissue inflammation. The aim of this study was to compare these techniques in patients with AAA.

Materials and methods: Fifteen patients with asymptomatic AAA with diameter 46 ± 7 mm underwent PET-CT with ^{18}F-FDG, and T2*-weighted MRI before and 24 hours after administration of USPIO. The PET-CT and MRI data were then co-registered. Standardised uptake values (SUVs) were calculated to measure ^{18}F-FDG activity, and USPIO uptake was determined using the change in R2*. Comparisons between the techniques were made using a quadrant analysis and a voxel-by-voxel evaluation.

Results: When all areas of the aneurysm were evaluated, there was a modest correlation between the SUV on PET-CT and the change in R2* on USPIO-enhanced MRI ($n = 70{,}345$ voxels; $r = .30$; $p < .0001$). Although regions of increased ^{18}F-FDG and USPIO uptake co-localised on occasion, this was infrequent (kappa statistic 0.074; 95% CI 0.026–0.122). ^{18}F-FDG activity was commonly focused in the shoulder region whereas USPIO uptake was more apparent in the main body of the aneurysm. Maximum SUV was lower in patients with mural USPIO uptake.

Conclusions: Both ^{18}F-FDG PET-CT and USPIO-MRI uptake identify vascular inflammation associated with AAA. Although they demonstrate a modest correlation, there are distinct differences in the pattern and distribution of uptake, suggesting a differential detection of macrophage glycolytic and phagocytic activity respectively.

Article history: Received 11 March 2015, Accepted 12 December 2015, Available online 23 February 2016

Keywords: Abdominal aortic aneurysms, Magnetic resonance imaging, Positron emission tomography, Computed tomography

INTRODUCTION

Recent advances in imaging modalities have generated considerable interest in novel molecular and cellular techniques. In contrast to anatomical and structural approaches, molecular and cellular imaging targets the activity of specific biochemical and cellular processes to provide insight into the aetiology, biology, and pathogenesis of diseased states. Moreover, this has the potential to refine the diagnosis and risk stratification of cardiovascular disease as well as to assess responses to specific therapeutic interventions.[1–5] A combination of morphological imaging with molecular imaging has proven a particularly useful approach.

^{18}F-Fludeoxyglucose (^{18}F-FDG) is used to image metabolically active cells with combined positron emission and computed tomography (PET-CT). ^{18}F-FDG accumulates in all

[e] These authors contributed equally.

* Corresponding author. Centre for Cardiovascular Science, University of Edinburgh, Little France Crescent, Edinburgh EH16 4SB, UK.
E-mail address: olivia.mcbride@ed.ac.uk (O.M.B. McBride).

http://dx.doi.org/10.1016/j.ejvs.2015.12.018

cells and tissues that metabolise glucose, in direct proportion to their metabolic activity. In atherosclerotic arteries and those affected by vasculitides, ^{18}F-FDG uptake correlates with the degree of arterial inflammation and is reproducible.[6–8] Furthermore, ^{18}F-FDG uptake increases with the number of cardiovascular risk factors present, is predictive of future cardiovascular events,[9–11] and has been used as a biomarker to demonstrate the anti-inflammatory effects of statins and other novel therapies.[12–14] ^{18}F-FDG accumulates in the wall of abdominal aortic aneurysms (AAAs) and several studies have correlated uptake with aortic vessel wall inflammation on histology.[15–17] There is evidence to suggest that ^{18}F-FDG can discriminate between asymptomatic and symptomatic AAA, but its potential use as a marker of aneurysm expansion, progression, and rupture has yet to be established.[15–22]

Magnetic resonance imaging (MRI) with ultrasmall superparamagnetic particles of iron oxide (USPIO) is an alternative approach for detecting cellular inflammation.[23,24] Owing to their small particle size (diameter 10–30 nm), USPIO escape immediate recognition by the reticulo-endothelial system, persist in the bloodstream, and accumulate at sites of vascular inflammation. Here they undergo phagocytosis by tissue-resident macrophages within which they accumulate and are detectable on T2- and T2*-weighted MRI sequences. Within atheromatous plaques, USPIO uptake correlates with macrophage density, distinguishes stable from unstable carotid plaques, and is reduced following high-dose atorvastatin therapy.[25–27] USPIO uptake in the wall of AAAs has previously been demonstrated, where it co-localises with macrophages and is associated with a threefold higher AAA growth rate.[24]

Given that both ^{18}F-FDG PET and USPIO-enhanced MRI have been used to assess vascular inflammation in patients with AAA, the aim of this study was to compare ^{18}F-FDG PET and USPIO-enhanced MRI in patients with AAAs. Specifically, the spatial distribution and intensity of the inflammatory process using both techniques was assessed to determine whether they provided complementary or distinct insights into the pathology of AAAs.

MATERIALS AND METHODS

Subjects

Patients with asymptomatic AAA (diameter 30–55 mm on duplex ultrasound examination) were recruited from the aneurysm surveillance clinic at the Royal Infirmary of Edinburgh. Exclusion criteria were age $<$ 50 years, active systemic inflammatory or malignant disease, renal dysfunction (estimated glomerular filtration rate $<$ 30 mL/min, because of the risks of contrast induced renal dysfunction), hepatic cirrhosis (Child–Pugh score B or C, because of the contrast agent not having been studied in this group of patients), planned AAA surgery within 6 months of screening, any contraindication to MRI and insulin-dependent diabetes mellitus (due to the confounding of ^{18}F-FDG uptake with variable blood glucose concentrations). Studies were performed with the approval of the local research ethics committee, in accordance with the Declaration of Helsinki, and with the written informed consent of each participant.

All patients underwent a comprehensive baseline clinical assessment, including evaluation of their cardiovascular risk factor profile and recording of an abdominal ultrasound scan. ^{18}F-FDG PET-CT and USPIO-MRI data acquisition procedures are detailed in Methods I of the Supplementary Material.

Image analysis

Registration of PET and MRI images. The accuracy of PET-CT to Computed Tomography Aortogram (CTA) registration was confirmed by visual assessment, and minor intra-scan patient movement was corrected using a semi-automatic rigid 3D voxel registration protocol (Analyze 11.0, Mayo Clinic, Rochester, MN, USA). Registration of the MRI data allowed the excellent anatomical detail on the T2W images and the high sensitivity of T2*W images for iron to be utilised. All MR images were registered to the pre-contrast T2W image. The CTA and T2W MRI datasets were also co-registered. At the end of the registration process, the pre-USPIO T2*W MRI, the post-USPIO T2*W MRI, the CTA, and the PET-CT were all co-registered to enable direct comparison. All steps of registration used a semi-automatic rigid 3D voxel registration protocol that has been previously validated and published.[24] All outputs were manually checked and optimised as necessary. Two independent trained observers, who were experienced vascular surgeons who had developed the image analysis techniques, undertook the analyses. There was excellent inter-observer agreement with kappa statistics between 0.84 and 0.89, for all steps.

^{18}F-FDG quantification. The maximum standardised uptake value (SUV_{max}) was used to assess ^{18}F-FDG uptake in the aneurysm. The SUV is the decay-corrected tissue uptake divided by the injected dose per unit body weight and is a semi-quantitative dimensionless unit that has been previously validated and is a commonly used measure of tissue ^{18}F-FDG uptake.[5,28] The SUV in vascular structures can be heavily influenced by variability of ^{18}F-FDG activity in the blood pool. Therefore, the tissue-to-background ratio (TBR) was also calculated by dividing the tissue SUV_{max} by an averaged mean SUV in the blood pool, derived from five circular regions of interest in the centre of the inferior vena cava. An area of ^{18}F-FDG uptake was defined as positive if the SUV_{max} or TBR was $>$ 125% of the value obtained from an averaged SUV_{max} from five randomly selected regions in the non-aneurysmal descending thoracic aorta.[29,30]

USPIO quantification. Using validated in-house software built in the Matlab environment (Mathworks, Natick, MA, USA), all four echoes in the multi-echo T2*W sequence were combined to generate a T2* map in which the magnitude of each voxel represented the T2* value ($S(t) = S(0)\exp - (t/T2^*)$). USPIO uptake was detected using the change in T2* (or R2*; R2* = 1/T2*) following USPIO administration. We applied a validated image analysis

method previously published for ΔT2* thresholding of AAA-USPIO data in order to visually interpret and threshold the UPSIO T2*-weighted data.[24] Increasingly R2* (=1/T2*) are reported to provide a positive correlation between concentration of USPIO and increase in R2* values, facilitating more straightforward data interpretation and visualisation. Detailed USPIO quantification methodology is outlined in Methods II of the Supplementary Material.

The correlation between ^{18}F-FDG uptake and USPIO distribution was analysed using three methods: the signals in different regions of the aneurysm were compared by drawing regions of interest (ROI) around the wall and thrombus, then the co-localisation across the aneurysm as a whole using a voxel-by-voxel analysis was studied. Finally, a previously defined aneurysm classification system based on USPIO uptake on MRI[24] was compared with the mean SUV_{max} and TBR for the positive regions of ^{18}F-FDG uptake in each aneurysm.

Colour maps. Two independent observers, blinded to patient demographics and aneurysm size reviewed the ΔT2* colour maps and the fused PET-CT data. Each axial slice was divided into quadrants and each quadrant was defined as positive if it included at least one region of increased USPIO or ^{18}F-FDG uptake, or negative if it did not. On the ΔT2* colour maps, significant regions of USPIO accumulation were defined as consisting of at least 10 contiguous voxels with ΔT2* above the threshold of 59%.[24] On the PET-CT scans, ROI were drawn around areas of maximum uptake in the wall and thrombus of the aneurysm and defined as positive if the SUV_{max} or TBR was $>$ 125% of the value obtained from an averaged SUV_{max} from five randomly selected regions in the non-aneurysmal descending thoracic aorta.

In order to define the area of the aneurysm where there was increased uptake of USPIO or ^{18}F-FDG, the aneurysm was divided in the axial plane into three distinct regions: on MRI the shoulder region extended one slice (5 mm) above and below the point at which the aorta last measured $\leq$ 30 mm in diameter, whereas on PET-CT, two slices (6 mm) were considered. The bifurcation region was defined in an identical way but from the point where the aneurysm reduced in diameter to $\leq$ 30 mm. The area between these two points was defined as the main body of the aneurysm.

Voxel-by-voxel analysis. The MR images were reconstructed by down-sampling to achieve equivalent voxel sizes with the corresponding PET images. A ROI encompassing the entire aortic wall and thrombus was drawn on each slice of the pre-contrast T2W image. These ROIs were then applied to the PET images and to the calculated ΔR2* colour maps. This enabled a quantitative voxel-by-voxel analysis of USPIO and ^{18}F-FDG uptake.

Aneurysm classification. We have previously shown that mural USPIO uptake predicts expansion; therefore, aneurysms were classified into three predefined groups by two independent blinded observers: Group 1, no mural or thrombus USPIO uptake, except for isolated periluminal enhancement; Group 2, diffuse USPIO uptake, distinct from the periluminal thrombus and aortic wall; and Group 3 focal areas (with at least 10 contiguous voxels) of USPIO uptake within the aortic wall of the aneurysm, distinct from the periluminal area and thrombus.[24] PET activity in regions of increased uptake was then compared across these three groups.

A schematic outlining the image analysis techniques undertaken can be found in Methods III of the Supplementary Material.

Statistical analysis

Normally distributed continuous variables were expressed as mean ± standard deviation. Non-parametric data were presented as median with interquartile ranges. Correlations between normally distributed data were performed using Pearson's correlation. Comparisons were undertaken with paired or unpaired Student's *t*-tests as appropriate. A two-sided $p < .05$ was regarded as statistically significant. Statistical analysis was performed with the use of Graph Pad Prism version 5 (GraphPad Software Inc., La Jolla, CA USA).

RESULTS

Fifteen predominantly elderly men with multiple cardiovascular risk factors and a mean AAA diameter of 46 mm (range 34–55 mm) participated in the study (Table 1). All patients were asymptomatic and had fusiform aneurysms confined to the abdominal aorta. ^{18}F-FDG PET-CT and USPIO-enhanced MRI scans were performed a median of 7 days apart. PET imaging of the abdomen was undertaken a median of 92 (IQR, 89–97) minutes after injection of 237 ± 16 MBq of ^{18}F-FDG. The effective radiation from participation in the study was 10.8 mSv using a conversion

Table 1. Baseline characteristics of patients with abdominal aortic aneurysm ($n = 15$).

Age (years)	73 ± 4
Male:female	13:2
% Male	87%
Maximum anteroposterior diameter of AAA (mm)	46 (range 34–55)
Cardiovascular history	
Coronary artery disease	5 (33%)
Stroke or transient ischemic attack	2 (13%)
Peripheral vascular disease	2 (13%)
Risk factors	
Current smoking habit	6 (40%)
Previous smoking habit	8 (60%)
Diabetes mellitus	1 (7%)
Hypertension	10 (67%)
Hypercholesterolemia	15 (100%)
Medications	
Antiplatelet agent	12 (80%)
Statin	13 (87%)
β-Blocker	6 (40%)
ACE inhibitor/ARB[a]	8 (53%)
Other Anti-hypertensive	2 (13%)

[a] Angiotensin converting enzyme (ACE) inhibitor or angiotensin II receptor blocker (ARB).

factor of 0.014 mSv/mGy cm. The administration of ^{18}F-FDG and USPIO was well tolerated with no adverse events.

^{18}F-FDG uptake

Increased ^{18}F-FDG uptake was observed within the wall of 13 of the 15 AAAs. In total there were 42 regions of increased uptake and all were diffuse and involved the wall. Although it was not possible to resolve whether this uptake localised to the aneurysm wall or the thrombus, the majority were observed in the shoulder region of the aneurysm (25/42, 60%), with a third (14/42) occurring within the main body of the aneurysm and the remainder in close proximity to the bifurcation (3/42). There was increased uptake in the peri-luminal zone of the thrombus in all patients.

USPIO uptake

All AAA demonstrated uptake of USPIO but focal areas of mural USPIO were primarily confined to the main body of the aneurysm (146/271, 54%), with 28% (75/271) located in the shoulder region and 19% (50/271) adjacent to the bifurcation (Table 2). In keeping with our previous study,[24] all patients had USPIO uptake in the periluminal area, representing a movement of particles directly into the thrombus from the blood pool.

Comparison between ^{18}F-FDG and USPIO uptake

When all areas of the aneurysm were considered, there was a modest correlation between the SUV on PET-CT and the absolute change in R2* on MRI ($r = .30$; 95% CI 0.29—0.31, $p < .0001$; Fig. 1).

In general, the main thrombus (excluding the peri-luminal region) did not uptake ^{18}F-FDG or USPIO. In contrast, local inflammation within the wall was readily identifiable but was not reflected by a change in T2* or R2* value in the whole aneurysm because of the associated dilutional effect of the thrombus.

Classification of AAA according to ^{18}F-FDG or USPIO uptake using the quadrant technique was consistent and reproducible with excellent inter-observer agreement and a kappa statistic of 0.87 for ^{18}F-FDG and 0.85 for USPIO. On occasion, areas of increased USPIO and ^{18}F-FDG uptake co-localised to the same quadrant in the aortic wall, although regions of USPIO uptake without corresponding ^{18}F-FDG uptake were also commonly seen (Fig. 2). Overall, co-localisation of areas of increased USPIO and ^{18}F-FDG uptake were poor (kappa statistic 0.074; 95% CI 0.026—0.122) and there were more areas of increased uptake identified on MRI than on PET-CT (Table 3). Focal and discrete uptake of USPIO can be readily discerned on MRI, whereas there was more diffuse and ill-defined uptake of ^{18}F-FDG involving both the wall and the thrombus on PET-CT.

Based on USPIO uptake, four patients were classified into Group 3 and 11 into Groups 1 and 2. SUV_{max} and TBR appeared to be lower in those classified as Group 3 than in those in Groups 1 and 2, but this did not reach statistical significance ($p = .7884$, 95% CI −2.181 to 1.690; Fig. 1). There was no correlation between the grouping classification and the maximum absolute change in R2* ($p = .4123$, 95% CI −86.99 to 37.98).

DISCUSSION

In comparing ^{18}F-FDG PET-CT with USPIO-enhanced MRI in patients with AAA, we have identified a modest correlation between these two imaging modalities but a number of key differences. In particular, activity detected with these two techniques appears to be concentrated in different regions of the aneurysm: largely in the shoulder region with ^{18}F-FDG and in the body of the aneurysm using USPIO. We believe that this reflects the different elements of inflammatory activity detected by these two approaches, with PET-CT providing information related to glycolysis and USPIO information on phagocytosis. Further studies are now required to assess which modality will have the greatest predictive power to determine aneurysm growth and clinical outcome.

Inflammatory cells have a key role in the development and progression of abdominal aortic aneurysms.[17] Histopathologically, the aneurysmal aortic wall is characterised by focal medial neovascularisation, infiltration of inflammatory cells (principally macrophages and lymphocytes), and fragmentation of elastin and collagen fibres within the extracellular matrix. Both ^{18}F-FDG and USPIO imaging aim to detect and quantify the inflammatory cellular component and it is therefore encouraging that a modest correlation between these two measures was observed in this study, confirming that ultimately both identify vascular inflammation, albeit through differing pathways.

Vascular inflammatory cells are metabolically active and take up ^{18}F-FDG in an insulin-insensitive manner. Therefore,

Table 2. Qualitative evaluation of ^{18}F-fludeoxyglucose (FDG) uptake on positron emission tomography and computed tomography (PET-CT) compared to ultrasmall superparamagnetic particles of iron oxide (USPIO) uptake on magnetic resonance imaging (MRI).

	^{18}F-FDG PET-CT	USPIO MRI
Spatial resolution	4—6 mm	2 mm (subject to field of view)
Periluminal enhancement	Present	Present
Region of uptake	Predilection for shoulder region	Predilection for main body of aneurysm
Definition of uptake	> 125% of the averaged SUV_{max} from five randomly selected regions in the non-aneurysmal descending thoracic aorta	10 contiguous voxels with % change in T2* ≥59%
Functional assessment	Glycolytic activity	Phagocytic activity
Ionising radiation	Yes	No

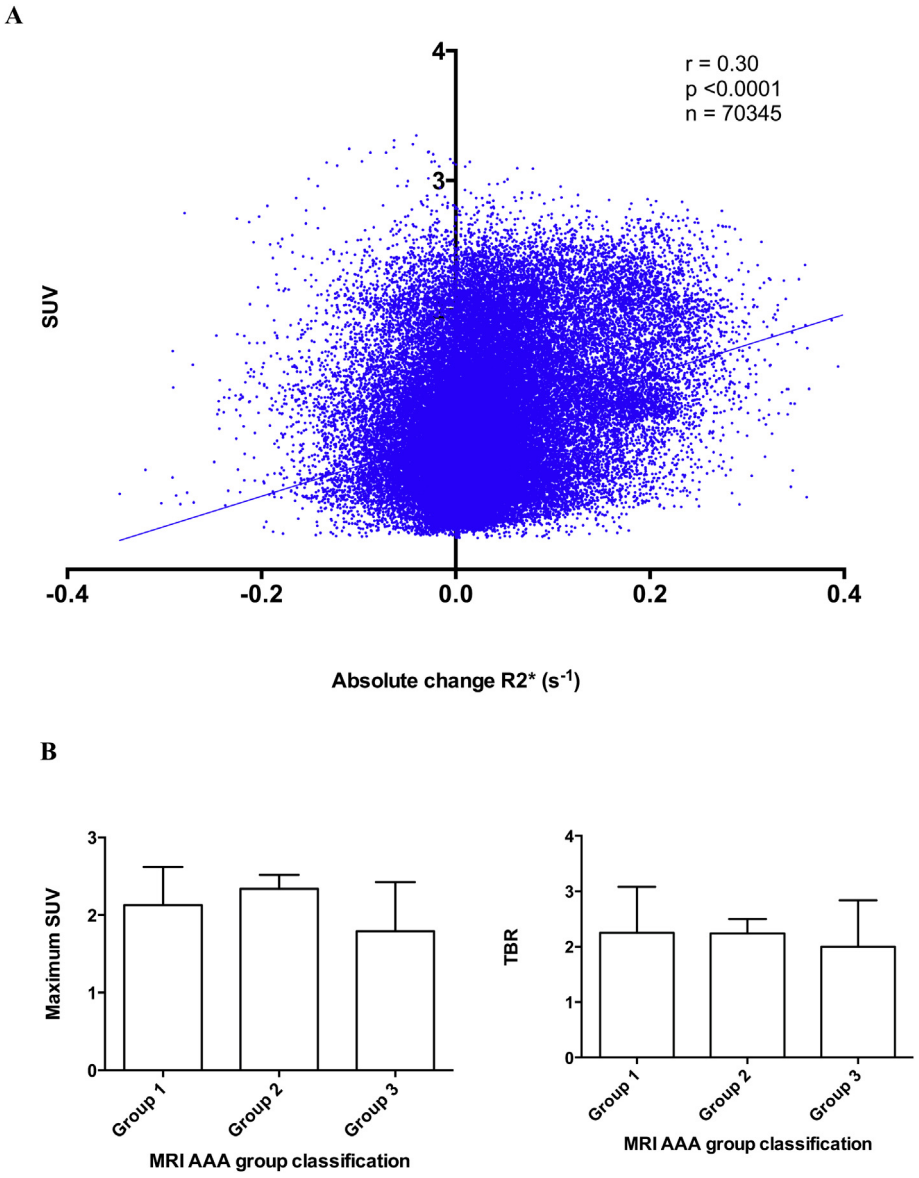

Figure 1. (A.) Comparison of standard uptake value (SUV) and absolute change in R2* in the wall of the abdominal aortic aneurysm (AAA). When the thrombus and wall of the aneurysm are considered there is a modest correlation between the SUV and the absolute change in R2* ($r = 0.30$). (B) MRI group classification compared to maximum SUV (SUV_{max}) and tissue-to-background ratio (TBR) in the wall of the AAA. There was no significant difference between the SUV_{max} ($p = .4696$, 95% CI −1.682 to 0.8194) or TBR ($p = .7884$, 95% CI −2.181 to 1.690) of patients in Groups 1 and 2 and those in Group 3.

^{18}F-FDG uptake in the fasted state has been proposed as a marker of risk for aneurysm progression and rupture with higher uptake associated with inflammation, aortic wall instability, and clinical symptoms.[15,18] However, the role of ^{18}F-FDG PET-CT in AAA disease remains controversial. Recent data have suggested that vascular ^{18}F-FDG activity may relate to more than simply macrophage burden,[31] with several studies identifying high lymphocyte counts and leucocytes[15,17,32] within the aortic wall and implicating hypoxia as an important driver to ^{18}F-FDG uptake.[33] Furthermore, although several small studies have demonstrated the ability of ^{18}F-FDG to discriminate between symptomatic and asymptomatic AAA,[15–18,21] a number of published studies have failed to verify these observations. Palombo et al.[34] showed ^{18}F-FDG uptake was low in asymptomatic AAAs, with a diameter close to surgical indications (mean diameter, 4.9 cm), perhaps reflecting decreased cell density in large AAAs. Tegler et al.[32] found no relationship between ^{18}F-FDG uptake and asymptomatic (small or large) AAAs versus controls and no correlation between histology and uptake. Similarly, Kotze et al.[20] found an inverse relationship between ^{18}F-FDG uptake and future growth rate of AAA.

USPIO-enhanced MRI has been used to explore a number of inflammatory conditions, including atherosclerotic plaques and abdominal aortic aneurysms.[23–25,27] USPIO are taken up by inflammatory phagocytic cells, particularly macrophages, and accumulate at sites of cellular

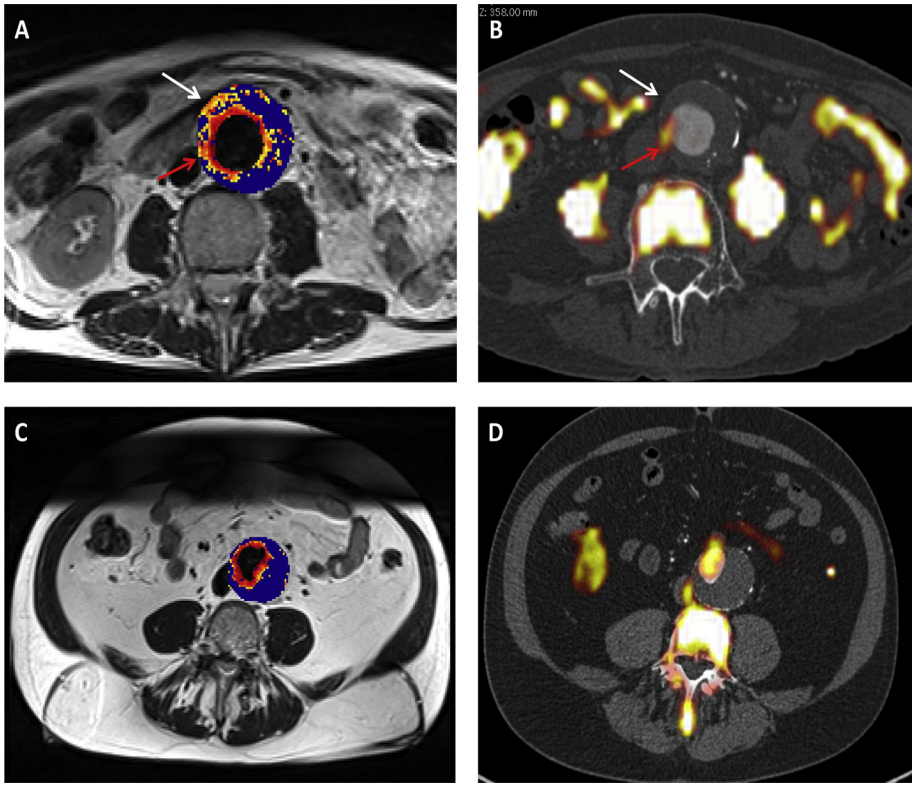

Figure 2. (A,B) Representative magnetic resonance imaging (MRI) (A) and fused positron emission tomography and computed tomography (PET-CT) (B) scans from the same patient with an abdominal aortic aneurysm (AAA). Ultrasmall superparamagnetic particles of iron oxide (USPIO) uptake, defined by percentage change in T2* is demonstrated using a colour scale. Changes in T2* value over the threshold (59%) are presented on a graduated (yellow-red) colour scale and data below the threshold appears blue. Corresponding ^{18}F-fludeoxyglucose (FDG) activity (red arrow) can be seen in B. Differences in the location of regions of uptake between the techniques are apparent, as marked by the white arrow. (C,D) are corresponding MRI and fused PET-CT slices from the same patient who has no USPIO or ^{18}F-FDG uptake in the wall of the AAA, with uptake limited to the peri-luminal area.

inflammation at sufficient concentrations to cause signal changes on MRI. In addition, histological examination of excised tissue, including aneurysm tissue, has confirmed the co-localisation and uptake of USPIO in areas of macrophage infiltration.[24,35–37]

We speculate that USPIO and ^{18}F-FDG uptake represent distinct markers of vascular inflammation that correspond to differing inflammatory and macrophage activities. Clearly, USPIO uptake is a measure of ongoing phagocytic activity of tissue-resident macrophages and potentially neutrophils, whereas ^{18}F-FDG reflects glucose utilisation by cells with high metabolic requirements including the cells implicated in vascular inflammation.[38] Moreover there is evidence that the two techniques target different macrophage subsets. Macrophages exist in varying polarised states and have different roles in vascular tissue. M1 macrophages are considered more destructive, promoting the destabilisation and rupture of atherosclerotic plaques, whereas phagocytosis is more important in the role of M2 macrophages stimulating reparative processes, mediated by the production of anti-inflammatory cytokines and the suppression of pro-inflammatory signalling.[39] It has been suggested that ^{18}F-FDG and USPIO uptake may be able to differentiate these two distinct M1 and M2 macrophage sub-populations respectively.[40] In this study, the majority of ^{18}F-FDG uptake was identified in the shoulder region of the aneurysm, an area of high biomechanical stress,[41,42] with a particular tendency to rupture: perhaps related to a destructive macrophage phenotype in this area.

Even though it has been demonstrated that our USPIO aneurysm classification identifies aneurysms likely to progress and dilate (Group 3; distinct mural USPIO uptake) we found no correlation between this classification and ^{18}F-FDG uptake nor the maximum absolute change in R2*. This supports the suggestion that it is the location of USPIO

Table 3. Quadrant analysis of the aneurysm wall: Regions of uptake identified by magnetic resonance imaging (MRI) and positron emission tomography and computed tomography (PET-CT). kappa statistic = 0.074 (95% C.I. 0.026—0.122), representing a poor strength of agreement.

		PET-CT		
MRI		Regions of uptake	No regions of uptake	Total
	Regions of uptake	70	353	423
	No regions of uptake	69	613	682
	Total	139	966	1015

uptake that is crucial, rather than the degree of USPIO uptake. However, the modest correlation that was demonstrated between maximum absolute change in R2* and SUV on a voxel-by-voxel basis supports the contention that these imaging modalities are both detecting elements of macrophage activity, namely phagocytosis and glucose metabolism.

Study limitations

There are important study limitations and technical considerations when interpreting our findings. We acknowledge that co-registration of the MRI and PET-CT datasets was challenging and cannot exclude partial or incomplete co-registration. Moreover, the limited in-plane resolution of PET-CT makes definition of the aortic wall and thrombus difficult and therefore challenging to locate the exact site of activity. Indeed this may also explain the increased ^{18}F-FDG uptake observed in the shoulder region, which is more prone to partial volume effects due to its angulation through the slice. This may reduce the sensitivity of the study in detecting ^{18}F-FDG or USPIO activity. However, as the thrombus uptakes little contrast agent, if thrombus was inadvertently included in the aortic wall assessment, this would lead to a tendency to under report uptake, thus our findings could be considered conservative. Additionally, there is no consensus or validated definition of quantitative significance values for ^{18}F-FDG or USPIO uptake and despite the excellent inter-observer reproducibility demonstrated in this study, this may contribute to the differences observed.

The contribution of statin therapy to the results of this study also cannot be excluded. To date there is only observational data showing AAA growth reduction with statins and mechanistic data are limited.[43,44] Although statin use has been shown to suppress AAA formation in animal models, this has not been translated to humans.[45,46] The use of statins in vascular patients to reduce cerebrovascular and cardiovascular mortality as well as in patients undergoing AAA surgery is well documented.[47,48] Consequently a clinical trial with and without statin therapy in AAA patients would be ethically challenging. The clinical trial was registered at ClinicalTrials.gov (NCT01749280)

Intra-individual correlation of histologic specimens from areas of minimum and maximum uptake of contrast would provide evidence of co-localisation of inflammatory activity but the practicalities of such are limited with the increase in endovascular abdominal aortic aneurysm repair (EVAR) and the ability to sample only tissue from the anterior portion of the aortic wall. Moreover, ex vivo ^{18}F-FDG uptake is limited by the need for fresh viable tissue, whereas USPIO uptake can only be assessed when undertaken in very close proximity to elective surgery.

This was a small study population that will require prospective evaluation in larger patient cohorts. Furthermore, this study was limited by the exclusion of AAA $\geq$ 55 mm as aneurysm growth and rupture is unpredictable and non-linear. Current guidelines suggest that surveillance with selective repair is the most appropriate management strategy.[49] However, as improvements in device technology for EVAR continues, this may change. Given this limited sample size, we were unable to assess the relationship between uptake of either ^{18}F-FDG or USPIO with AAA growth rates or clinical outcome. A number of small studies have demonstrated the ability of ^{18}F-FDG to differentiate between symptomatic and asymptomatic AAAs[15–18,21] and a recent study has suggested an association between ^{18}F-FDG activity and future clinical events.[41] A pilot study of 29 patients demonstrated that USPIO uptake in the wall of AAA is associated with accelerated expansion rates.[24] Further datasets with long-term follow-up are therefore required to undertake more complete evaluation of these promising imaging approaches.

An observational surveillance trial is currently underway at the centre to assess the relationship between mural USPIO uptake and subsequent clinical outcomes, with the aim of improving risk stratification of patients with AAA: the MA3RS trial (MRI for AAA to predict rupture or surgery; ISRCTN76413758).

In conclusion, the correlation between ^{18}F-FDG PET-CT and USPIO-enhanced MRI to detect vascular inflammation in AAAs is modest and reflects the differing elements of macrophage activity that they detect: glycolysis and phagocytosis respectively. Whether the identification of this varying activity will impact on aneurysm growth rates or risk of aneurysm rupture will require larger longitudinal study.

COMPETING INTERESTS

None.

FUNDING

This research was supported by grants from the National Institutes of Health Research (NIHR) Efficacy and Mechanism Evaluation Programme (11/20/03), the British Heart Foundation (PG/09/083) and the Evelyn Trust (09/22). Dr. McBride is supported by the Academic Department of Military Surgery and Trauma, Royal Centre for Defence Medicine. Dr. Joshi is supported by Chief Scientist Office (ETM/160). Dr. van Beek is supported by the Scottish Imaging Network — a Platform of Scientific Excellence. The work of Dr. Rudd is part-supported by the NIHR Cambridge Biomedical Research Centre, the British Heart Foundation and the Wellcome Trust. Dr. Newby is supported by the British Heart Foundation (CH/09/002). The Wellcome Trust Clinical Research Facility and the Clinical Research Imaging Centre are supported by National Health Service Research Scotland through National Health Service Lothian.

ACKNOWLEDGEMENTS

The authors are grateful to the Wellcome Trust Clinical Research Facility and the Clinical Research Imaging Centre for their help with this study.

APPENDIX A. SUPPLEMENTARY MATERIAL

Supplementary material related to this article can be found at http://dx.doi.org/10.1016/j.ejvs.2015.12.018

REFERENCES

1 Jaffer FA, Libby P, Weissleder R. Molecular imaging of cardiovascular disease. *Circulation* 2007;**116**:1052—61.

2 Jaffer FA, Libby P, Weissleder R. Optical and multimodality molecular imaging: insights into atherosclerosis. *Arterioscler Thromb Vasc Biol* 2009;**29**:1017—24.

3 Choudhury RP, Fisher EA. Molecular imaging in atherosclerosis, thrombosis, and vascular inflammation. *Arterioscler Thromb Vasc Biol* 2009;**29**:983—91.

4 Nahrendorf M, Keliher E, Marinelli B, Leuschner F, Robbins CS, Gerszten RE, et al. Detection of macrophages in aortic aneurysms by nanoparticle positron emission tomography-computed tomography. *Arterioscler Thromb Vasc Biol* 2011;**31**:750—7.

5 Rudd JHF, Warburton EA, Fryer TD, Jones HA, Clark JC, Antoun N, et al. Imaging atherosclerotic plaque inflammation with [^{18}F]-fluorodeoxyglucose positron emission tomography. *Circulation* 2002;**105**:2708—11.

6 Rudd JHF, Myers KS, Bansilal S, Machac J, Rafique A, Farkouh M, et al. (18)Fluorodeoxyglucose positron emission tomography imaging of atherosclerotic plaque inflammation is highly reproducible: implications for atherosclerosis therapy trials. *J Am Coll Cardiol* 2007;**50**:892—6.

7 Tawakol A, Migrino RQ, Hoffman U, Abbara S, Houser S, Gewirtz H, et al. Noninvasive in vivo measurement of vascular inflammation with F-18 fluorodeoxyglucose positron emission tomography. *J Nucl Cardiol* 2005;**12**:294—301.

8 Tawakol A, Migrino RQ, Bashian GG, Bedri S, Vermylen D, Cury RC, et al. In vivo 18F-fluorodeoxyglucose positron emission tomography imaging provides a noninvasive measurement of carotid plaque inflammation in patients. *J Am Coll Cardiol* 2006;**48**:1818—24.

9 Rominger A, Saam T, Wolpers S, Cyran CC, Schmidt M, Foerster S, et al. ^{18}F-FDG PET/CT identifies patients at risk for future vascular events in an otherwise asymptomatic cohort with neoplastic disease. *J Nucl Med* 2009;**50**:1611—20.

10 Rudd JHF, Myers KS, Bansilal S, Machac J, Woodward M, Fuster V, et al. Relationships among regional arterial inflammation, calcification, risk factors, and biomarkers: a prospective fluorodeoxyglucose positron-emission tomography/computed tomography imaging study. *Circ Cardiovasc Imaging* 2009;**2**:107—15.

11 Tahara N, Kai H, Nakaura H, Mizoguchi M, Ishibashi M, Kaida H, et al. The prevalence of inflammation in carotid atherosclerosis: analysis with fluorodeoxyglucose-positron emission tomography. *Eur Heart J* 2007;**28**:2243—8.

12 Tahara N, Kai H, Ishibashi M, Nakaura H, Kaida H, Baba K, et al. Simvastatin attenuates plaque inflammation: evaluation by fluorodeoxyglucose positron emission tomography. *J Am Coll Cardiol* 2006;**48**:1825—31.

13 Fayad ZA, Mani V, Woodward M, Kallend D, Abt M, Burgess T. dal-PLAQUE Investigators. Safety and efficacy of dalcetrapib on atherosclerotic disease using novel non-invasive multimodality imaging (dal-PLAQUE): a randomised clinical trial. *Lancet* 2011;**378**:1547—59.

14 Tawakol A, Fayad ZA, Mogg R, Alon A, Klimas MT, Dansky H, et al. Intensification of statin therapy results in a rapid reduction in atherosclerotic inflammation: results of a multicenter fluorodeoxyglucose-positron emission tomography/computed tomography feasibility study. *J Am Coll Cardiol* 2013;**62**:909—17.

15 Reeps C, Essler M, Pelisek J, Seidl S, Eckstein H-H, Krause B-J. Increased 18F-fluorodeoxyglucose uptake in abdominal aortic aneurysms in positron emission/computed tomography is associated with inflammation, aortic wall instability, and acute symptoms. *J Vasc Surg* 2008;**48**:417—23.

16 Reeps C, Bundschuh RA, Pellisek J, Herz M, Marwick S, Schwaiger M, et al. Quantitative assessment of glucose metabolism in the vessel wall of abdominal aortic aneurysms: correlation with histology and role of partial volume correction. *Int J Cardiovasc Imaging* 2012;**29**:505—12.

17 Courtois A, Nusgens BV, Hustinx R, Namur G, Gomez P, Somja J, et al. 18F-FDG uptake assessed by PET/CT in abdominal aortic aneurysms is associated with cellular and molecular alterations prefacing wall deterioration and rupture. *J Nucl Med* 2013;**54**:1740—7.

18 Sakalihasan N, Hustinx R, Limet R. Contribution of PET scanning to the evaluation of abdominal aortic aneurysm. *Semin Vasc Surg* 2004;**17**:144—53.

19 Kotze CW, Menezes LJ, Endozo R, Groves AM, Ell PJ, Yusuf SW. Increased metabolic activity in abdominal aortic aneurysm detected by 18F-fluorodeoxyglucose. *Eur J Vasc Endovasc Surg* 2009;**38**:93—9.

20 Kotze CW, Groves AM, Menezes LJ, Harvey R, Endozo R, Kayani IA, et al. What is the relationship between ^{18}F-FDG aortic aneurysm uptake on PET/CT and future growth rate? *Eur J Nucl Med Mol Imaging* 2011;**38**:1493—9.

21 Truijers M, Kurvers HA, Bredie SJ, Oyen WJ, Blankensteijn JD. In vivo imaging of abdominal aortic aneurysms: increased FDG uptake suggests inflammation in the aneurysm wall. *J Endovasc Ther* 2008;**15**:462—7.

22 Nchimi A, Defawe O, Brisbois D, Broussaud TK, Defraigne J-O, Magotteaux P, et al. MR Imaging of iron phagocytosis in intraluminal thrombi of abdominal aortic aneurysms in humans. *Radiology* 2010;**254**:973—81.

23 Sadat U, Taviani V, Patterson AJ, Young VE, Graves MJ, Teng Z, et al. Ultrasmall superparamagnetic iron oxide-enhanced magnetic resonance imaging of abdominal aortic aneurysms-a feasibility study. *Eur J Vasc Endovasc Surg* 2011;**41**:167—74.

24 Richards JMJ, Semple SI, MacGillivray TJ, Gray C, Langrish JP, Williams M, et al. Abdominal aortic aneurysm growth predicted by uptake of ultrasmall superparamagnetic particles of iron oxide: a pilot study. *Circ Cardiovasc Imaging* 2011;**4**:274—81.

25 Trivedi RA, Mallawarachi C, U-King-Im J-M, Graves MJ, Horsley J, Goddard MJ, et al. Identifying inflamed carotid plaques using in vivo USPIO-enhanced MR Imaging to label plaque macrophages. *Arterioscler Thromb Vasc Biol* 2006;**26**:1601—6.

26 Tang TY, Muller KH, Graves MJ, Li ZY, Walsh SR, Young V, et al. Iron oxide particles for atheroma imaging. *Arterioscler Thromb Vasc Biol* 2009;**29**:1001—8.

27 Morishige K, Kacher DF, Libby P, Josephson L, Ganz P, Weissleder R, et al. High-resolution magnetic resonance imaging enhanced with superparamagnetic nanoparticles measures macrophage burden in atherosclerosis. *Circulation* 2010;**122**:1707—15.

28 Dweck MR, Jones C, Joshi NV, Fletcher AM, Richardson H, White A, et al. Assessment of valvular calcification and inflammation by positron emission tomography in patients with aortic stenosis. *Circulation* 2012;**125**:76—86.

29 Dweck MR, Chow M, Joshi NV, Williams MC, Jones C, Fletcher AM, et al. Coronary arterial ^{18}F-sodium fluoride uptake: a novel marker of plaque biology. *J Am Coll Cardiol* 2012;**59**:1539—48.

30 Joshi NV, Vesey AT, Williams MC, Shah AS, Calvert PA, Craighead FH, et al. 18F-fluroide positron emission tomography for identification of ruptured and high-risk coronary

atherosclerotic plaques: a prospective clinical trial. *Lancet* 2014;**383**:705—13.
31 Defawe OD, Hustinx R, Defraigne JO, Limet R, Sakalihasan N. Distribution of F-18 fluorodeoxyglucose (F-18 FDG) in abdominal aortic aneurysm: high accumulation in macrophages seen on PET imaging and immunohistochemistry. *Clin Nucl Med* 2005;**30**:340—1.
32 Tegler G, Ericson K, Sörensen J, Björck M, Wanhainen A. Inflammation in the walls of asymptomatic abdominal aortic aneurysms is not associated with increased metabolic activity detectable by 18-flurodeoxyglucose positron-emission tomography. *J Vasc Surg* 2012;**56**:802—7.
33 Folco EJ, Sheikine Y, Rocha VZ, Christen T, Shvartz E, Sukhova GK, et al. Hypoxia but not inflammation augments glucose uptake in human macrophages: implications for imaging atherosclerosis with 18fluorine-labeled 2-deoxy-D-glucose positron emission tomography. *J Am Coll Cardiol* 2011;**58**:603—14.
34 Palombo D, Morbelli S, Spinella G, Pane B, Marini C, Rousas N, et al. A positron emission tomography/computed tomography (PET/CT) evaluation of asymptomatic abdominal aortic aneurysms: another point of view. *Ann Vasc Surg* 2012;**26**:491—9.
35 Ruehm SG, Corot C, Vogt P, Kolb S, Debatin JF. Magnetic resonance imaging of atherosclerotic plaque with ultrasmall superparamagnetic particles of iron oxide in hyperlipidemic rabbits. *Circulation* 2001;**103**:415—22.
36 Kooi ME, Cappendijk VC, Cleutjens KBJM, Kessels AGH, Kitslaar PJEHM, Borgers M, et al. Accumulation of ultrasmall superparamagnetic particles of iron oxide in human atherosclerotic plaques can be detected by in vivo magnetic resonance imaging. *Circulation* 2003;**107**:2453—8.
37 Schmitz SA, Taupitz M, Wagner S, Wolf KJ, Beyersdorff D, Hamm B. Magnetic resonance imaging of atherosclerotic plaques using superparamagnetic iron oxide particles. *J Magn Reson Imaging* 2001;**14**:355—61.
38 Choke E, Cockerill G, Wilson WRW, Sayed S, Dawson J, Loftus I, et al. A review of biological factors implicated in abdominal aortic aneurysm rupture. *Eur J Vasc Endovasc Surg* 2005;**30**:227—44.
39 Shaikh S, Brittenden J, Lahiri R, Brown PAJ, Thies F, Wilson HM. Macrophage subtypes in symptomatic carotid artery and femoral artery plaques. *Eur J Vasc Endovasc Surg* 2012;**44**:491—7.
40 Satomi T, Ogawa M, Mori I, Ishino S, Kubo K, Magata Y, et al. Comparison of contrast agents for atherosclerosis imaging using cultured macrophages: FDG versus ultrasmall superparamagnetic iron oxide. *J Nuc Med* 2013;**54**:999—1004.
41 Nchimi A, Cheramy-Bien JP, Gasser TC, Namur G, Gomez P, Seidel L, et al. Multifactorial relationship between 18F-fluorodeoxy-glucose positron emission tomography signaling and biomechanical properties in unruptured aortic aneurysms. *Circ Cardiovasc Imaging* 2014;**7**:82—91.
42 Xu XY, Borghi A, Nchimi A, Leung J, Gomez P, Cheng Z, et al. High levels of 18F-FDG uptake in aortic aneurysm wall are associated with high wall stress. *Eur J Vasc Endovasc Surg* 2010;**39**:295—301.
43 Schlosser FJV, Tangelder MJD, Verhagen HJM, van der Heijden GJMG, Muhs BE, van der Graaf Y, et al. Growth predictors and prognosis of small abdominal aortic aneurysms. *J Vasc Surg* 2008;**47**:1127—33.
44 Karrowni W, Dughman S, Hajj GP, Miller FJ. Statin therapy reduces growth of abdominal aortic aneurysms. *J Investig Med* 2011;**59**:1239—43.
45 Kalyanasundaram A, Elmore JR, Manazer JR, Golden A, Franklin DP, Galt SW. Simvastatin suppresses experimental aortic aneurysm expansion. *J Vasc Surg* 2006;**43**:117—24.
46 Shiraya S, Miyake T, Aoki M, Yoshikazu F, Ohgi S, Nishimura M, et al. Inhibition of development of experimental aortic abdominal aneurysm in rat model by atorvastatin through inhibition of macrophage migration. *Atherosclerosis* 2009;**202**:34—40.
47 Kertai MD, Boersma E, Westerhout C, van Domburg R, Klein J, Bax JJ, et al. Association between long-term statin use and mortality after successful aortic aneurysm surgery. *Am J Med* 2004;**116**:96—103.
48 Schoulten O, Hoeks SE, Welten GM, Davignon J, Kastelein JJ, Vidakovic R. Effect of statin withdrawal on frequency of cardiac events after vascular surgery. *Am J Cardiol* 2007;**100**:316—20.
49 Chaikof EL, Brewster DC, Dalman RL, Makaroun MS, Illig KA, Sicard GA, et al. The care of patients with an abdominal aortic aneurysm: the Society for Vascular Surgery practice guidelines. *J Vasc Surg* 2009;**50**(Suppl. 4):S8—49.